Hiroyuki Fujiwara · Robert W. Collins
Editors

Spectroscopic Ellipsometry for Photovoltaics

Volume 1: Fundamental Principles and Solar Cell Characterization

Springer

Chapter 5
Dielectric Function Modeling

James N. Hilfiker and Tom Tiwald

Abstract Spectroscopic ellipsometry (SE) is commonly used to measure the optical constants of thin films and bulk materials. The optical constants vary with wavelength, which is referred to as dispersion. Rather than independently determine the optical constants at each wavelength, it is convenient to use an equation to describe their dispersion. A dispersion equation simplifies the description of the optical constants and improves the efficiency of data analysis. We begin this chapter by describing the optical constants, optical resonance, and the Kramers-Kronig relations. Different absorption phenomena are also briefly described. Many dispersion equations relate an optical resonance or absorption in terms of the complex dielectric function. Multiple resonance and absorption features can be summed to describe the overall dielectric function for the material. Finally, we review the common dispersion equations used for photovoltaic materials. The Cauchy and Sellmeier equations are used to describe transparent materials. The Lorentz, Harmonic, and Gaussian equations describe a resonant absorption. The Tauc-Lorentz and Cody-Lorentz were developed for amorphous semiconductors with dispersion features necessary to describe the optical functions near the bandgap energy. Additional dispersion equations are designed to describe the critical points in semiconductor band structure. We conclude this review with a description of polynomials, splines, and basis-splines, which are used to empirically match the optical functions of many materials.

5.1 Optical Absorption and Dispersion Features

In this section, we introduce the definitions for optical constants and consider the general shapes and origins of optical dispersion. We then introduce the Kramers-Kronig relations, which provide a formal connection between the real and

J. N. Hilfiker (✉) · T. Tiwald
J.A. Woollam Co., Inc., 645 M Street, Suite 102, Lincoln, NE 68508, USA
e-mail: jhilfiker@jawoollam.com

© Springer International Publishing AG, part of Springer Nature 2018

H. Fujiwara and R. W. Collins (eds.), *Spectroscopic Ellipsometry for Photovoltaics*,
Springer Series in Optical Sciences 212,
https://doi.org/10.1007/978-3-319-75377-5_5

jhilfiker@jawoollam.com

imaginary optical constants. Finally, we review the phenomena which lead to optical absorption at typical spectroscopic ellipsometry (SE) measurement frequencies.

5.1.1 Refractive Index and Dielectric Function

There are two common expressions for the optical constants of a material: the complex refractive index ($N = n - ik$) and the complex dielectric function ($\varepsilon = \varepsilon_1 - i\varepsilon_2$) [1]. While both were introduced in Chap. 3, we expand the discussion to describe their general shape and behavior. They are related by:

$$\varepsilon = \varepsilon_1 - i\varepsilon_2 = N^2 = (n - ik)^2 \tag{5.1}$$

with

$$\varepsilon_1 = n^2 - k^2 \tag{5.2a}$$

$$\varepsilon_2 = 2nk \tag{5.2b}$$

Because each term varies with wavelength, λ, we refer to $N(\lambda)$ and $\varepsilon(\lambda)$ as the *optical functions* of a material. The optical functions of amorphous germanium are graphed in Fig. 5.1, where N is plotted versus wavelength while ε is shown versus photon energy. Recall from (3.1) that photon energy is inversely related to wavelength. Both representations are acceptable and the graphs contain the same information, just modified by (5.1). In Sect. 5.3, we show that many dispersion equations describe ε versus photon energy because photon energy scales directly with frequency.

The complex refractive index generally describes how light is altered by interaction with a material. For example, the index of refraction, n, is related to the phase velocity (3.4). At an interface between two materials, the difference in the refractive index governs both the direction of the transmitted light (3.11) and the division of light amplitudes between reflection and transmission (3.15a–d). The extinction coefficient, k, is related to the absorption of light as it travels through a material (3.5) and (3.6).

The complex dielectric function also describes the interaction between light and materials. As light travels through a material, the light's oscillating electric fields create oscillating charge dipoles within atoms or between atoms. Each dipole reradiates an electromagnetic field, and will absorb some of the energy at certain oscillation frequencies. Each dipole field combines with the fields from other dipoles as well as the incident field resulting in the total macroscopic field within the material. The dielectric function, ε, describes the constitutive relation between

jhilfiker@jawoollam.com

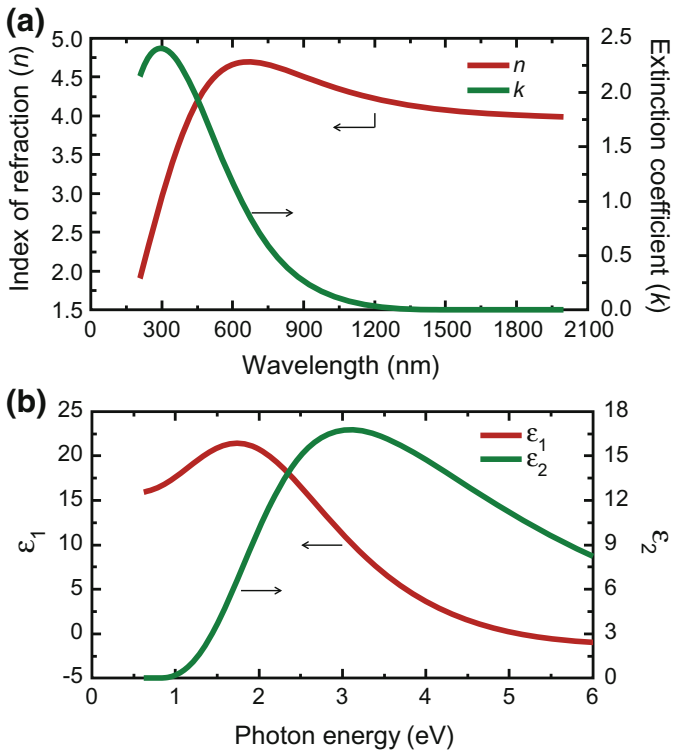

Fig. 5.1 **a** Refractive index versus wavelength and **b** dielectric function versus photon energy for amorphous germanium. While the graphs appear to be quite different, they contain the same information in different forms

the displacement field (**D**) (this is the total macroscopic field), the incident electric field (**E**), and the electric polarization (**P**) [2]:

$$\mathbf{D} = \varepsilon_0 \mathbf{E} + \mathbf{P} = \varepsilon\, \varepsilon_0 \mathbf{E} \tag{5.3}$$

where ε_0 is the permittivity of free space and ε is the relative dielectric constant. Since ε_0 is a constant, in this chapter we will concentrate on ε and simply call it the *dielectric constant*, dropping the term "relative". Rewriting (5.3) as

$$\varepsilon = \frac{\mathbf{D}}{\varepsilon_0 \mathbf{E}} = \frac{\varepsilon_0 \mathbf{E} + \mathbf{P}}{\varepsilon_0 \mathbf{E}} = 1 + \frac{\mathbf{P}}{\varepsilon_0 \mathbf{E}}. \tag{5.4}$$

we see that ε is a constant of proportionality for **D**/**E** and describes the contribution from **P**, which is a function of the volume density and strength of the dipoles contained within the material. The dipole response, and therefore **P**, depends on how quickly the **E**-fields oscillate. Thus ε is a function of frequency, $\varepsilon(\omega)$. The dipole response will also generally differ in both amplitude and phase from the oscillating **E**-fields of the incident light, making $\varepsilon(\omega)$ a complex value. Thus, the dielectric function contains a great deal of information about the material properties [2, 3].

jhilfiker@jawoollam.com

5.1.2 Resonance

We now consider how the dipole behavior affects the dielectric function. The dipoles are treated as a collection of classical oscillators, with a resonant frequency, driven by an externally applied harmonically oscillating force. This classical approach provides a reasonable description of the dielectric function shape versus frequency. It is a good starting model for the dipole-field interactions and energy absorption processes of materials. However it does not accurately describe band-gaps, absorption at critical points and other phenomena, which are more accurately described by semi-classical and quantum mechanical models.

Most SE measurements cover the ultraviolet (UV), visible, and near infrared (NIR) wavelengths. At these wavelengths, the light interacts primarily with electrons, as their mass is sufficiently small that they can respond to time-varying electric fields of a very high frequency. The time-varying electric field displaces the negatively-charged electron clouds relative to the heavier, positively-charged nuclei, forming dipoles as shown in Fig. 5.2a. The dipoles oscillate at the same frequency as the E-fields of incoming light; and in turn they reradiate light at that same frequency but with a phase and amplitude that is generally different than the incident field.

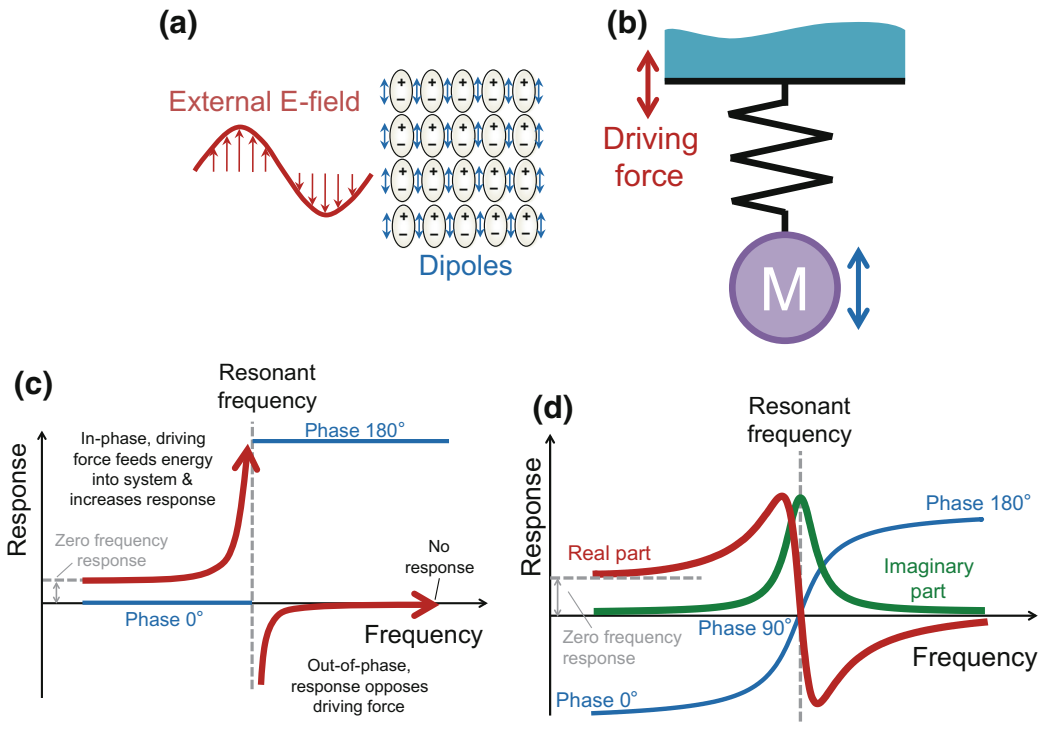

Fig. 5.2 **a** An oscillating electric field induces oscillating dipoles within a material. **b** A mass on a spring responds to an external driving force. **c** The frequency response of a lossless system and **d** the frequency response of a lossy system

jhilfiker@jawoollam.com

This phenomenon has many similarities to a mechanically resonant system driven by an external, harmonic oscillating force, such as the mass on a spring being driven at a specific frequency in Fig. 5.2b. Classical resonant systems are discussed in elementary physics textbooks, but we repeat a few concepts here that help describe the overall shape of a dielectric function. The frequency response of any resonant system can be described as a complex function, as shown in Figs. 5.2c, d for lossless and lossy systems, respectively. The real part represents the portion of the response that is in-phase with the driving force (when positive), or 180° out-of-phase with the driving force (when negative). The imaginary part represents the portion of the response that is 90° out-of-phase with the driving force. The imaginary part is also proportional to the energy loss at a given frequency.

When a zero frequency (static) force is applied, the system responds in the direction of the force, and the response function (in our case, the dipole displacement) is positive and real. The strength of the response depends upon the system particulars, such as mass, strength of the restoring force, and so on. As the applied force begins to oscillate at low frequencies, the real part of the response increases because the response and force are exactly in-phase (lossless system) or mostly in-phase (lossy system); therefore the driving force adds to the response.

In a lossless system (Fig. 5.2c), the response function is always real-valued because the phase is either 0° or 180°. As the frequency increases from zero to the resonant frequency, the response approaches positive infinity (and the phase remains zero). At the resonant frequency, the phase of the response abruptly transitions to 180°, such that it is out-of-phase with the force and the response becomes infinitely negative. As the driving frequency increases beyond the resonant frequency the response becomes smaller and smaller, because the force changes direction faster than the system can respond.

A lossy system will absorb energy, so the response remains finite at all frequencies (Fig. 5.2d). At low frequencies the response function of a lossy system looks very similar to that of a lossless system: the real part is positive and increases with frequency, and the imaginary part is nearly zero. As the frequency increases, the phase of the response lags further and further behind the driving force, which means they are more and more in opposition. At some frequency the driving force opposition is sufficiently large that the real part of the response reaches a maximum and begins to decrease. At about the same frequency, the imaginary part increases sharply. At the resonant frequency the real part of the response is zero, the imaginary part reaches a maximum, and the phase lag is 90°. Beyond the resonant frequency, the real part becomes more negative until at some point the force changes faster than the system can respond. The imaginary part declines from its maximum. At frequencies significantly higher than resonance, both the real and imaginary parts approach zero.

The dielectric function, ε, has a similar form to the frequency response of a classical oscillator. This is because the oscillating dipole displacements give rise to the polarization $\mathbf{P}$, which means that $\mathbf{P}$ has the same form as the response functions shown in Fig. 5.2c, d. Since ε is a function of $\mathbf{P}$ (5.4), it also takes on a similar

jhilfiker@jawoollam.com

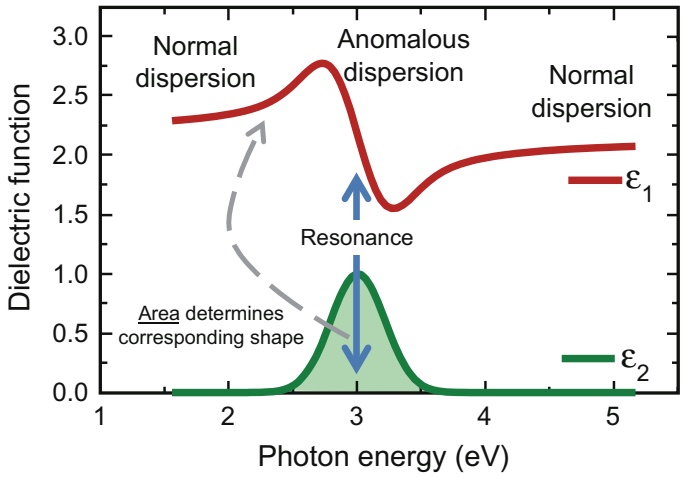

Fig. 5.3 Typical resonance absorption with normal and anomalous dispersion regions. The dispersion goes hand-in-hand with the absorption to maintain causality. Kramers-Kronig relations show that the area integrated under the ε_2 curve corresponds to the shape of the ε_1 curve

form. As an example, the dielectric function for transparent spectral regions is often modeled using a lossless dielectric function that looks very similar to Fig. 5.2c. We shall discuss this type of function when we consider the Sellmeier relation in Sect. 5.3.1.

For absorbing materials, the response function will look very similar to the ε_1 and ε_2 as shown in Fig. 5.3. Note the strong similarities between Figs. 5.2d and 5.3. The ε is usually described as a function of photon energy (in electron volts or eV), which is directly proportional to the electromagnetic field oscillation frequency. The energy loss, or light absorption, goes hand-in-hand with the optical dispersion and leads to regions of normal and anomalous dispersion. *Normal dispersion* describes the increasing ε_1 value as photon energy (or frequency) increases. Normal dispersion occurs at all photon energies where the absorption of light is negligible ($\varepsilon_2 \sim 0$). At energies where the material absorbs light, the slope of ε_1 becomes negative and its value decreases with increasing energy. This is referred to as *anomalous dispersion*. In Fig. 5.3, ε_2 reaches a peak at the resonant condition of 3 eV and we see that ε_1 has a negative slope. The actual shapes of ε_1 and ε_2 are related, as will be discussed in the next section.

5.1.3 Kramers-Kronig Relations

The Kramers-Kronig (KK) relations establish a physical connection between ε_1 and ε_2 as [4]:

$$\varepsilon_1(E) = 1 + \frac{2}{\pi} P \int_0^\infty \frac{E' \varepsilon_2(E')}{E'^2 - E^2} \mathrm{d}E' \tag{5.5a}$$

jhilfiker@jawoollam.com

$$\varepsilon_2(E) = -\frac{2E}{\pi} P \int_0^{\infty} \frac{\varepsilon_1(E')}{E'^2 - E^2} \mathrm{d}E' \tag{5.5b}$$

where P is the principal part of the integral and E is the photon energy of the light. Please note that these equations define the dielectric function as $\varepsilon = \varepsilon_1 + i\varepsilon_2$. These equations are the result of causality, where the response cannot precede the cause. In our case the material dipole response and absorption must occur after the electric field is applied. The KK relations help illustrate a few physical properties of the optical functions.

1. The shapes of ε_1 and ε_2 are not independent. The KK relations provide the connection between their values. In theory, if we can describe one function (either ε_1 or ε_2), the second can be calculated. In practice, we can calculate the general shape of the corresponding function but are often prevented from the exact calculation (see #3).
2. The KK relations involve integration, thus the ε_1 shape depends on the area under the ε_2 curve, as shown in Fig. 5.3. Simply stated, absorption causes anomalous dispersion and the larger the area under ε_2, the larger the effect on ε_1.
3. The KK relations integrate over *all* photon energies. Thus, ε_1 at a given energy is affected by ε_2 at all energies. In practice, we can generally describe ε_2 within our measured spectral range. However, absorptions outside the measured spectral range also affect the ε_1 curve. Thus, the KK calculation does not necessarily provide an exact match to our desired ε_1 curve. However, it does provide the correct general shape. We discuss this issue in Sect. 5.2.2.

The KK relations are very important during SE data analysis. They help limit the possible optical functions to only those that are physically plausible. They also greatly reduce the number of free parameters needed to describe complex optical functions. This is generally accomplished by using equations to describe the shape of ε_2 and then calculating ε_1 from (5.5a). For this reason, we consider the mechanisms which produce absorption within a material in the next section.

5.1.4 Absorption Phenomena

We consider three absorption phenomena which may affect the material optical functions at typical SE wavelengths: electronic transitions, free-carrier absorption and vibrational absorption.

jhilfiker@jawoollam.com

5.1.4.1 Electronic Transitions

Most SE measurements use wavelengths from the UV to the NIR. At these wavelengths, the most common absorptions involve electrons. Electronic transitions occur when light of the correct photon energy causes an electron to transition between energy bands, which is why these are also called interband transitions. This absorption mechanism is commonly found in dielectrics, organics, and semiconductors. It also occurs in the UV and visible optical functions of metals, although it is less obvious because the absorptions from electronic transitions can be masked by the effects of conductivity. Electronic transitions also form the basis for the photovoltaic process—light is absorbed by the material and transformed into electrical energy. Thus, absorption from electronic transitions is of significant interest for PV materials. SE can be used to determine which wavelengths (or photon energies) will be absorbed and the amount of absorption.

The bandgap energy is the minimum energy required to initiate electronic transitions between bands. Recall that the photon energy of light is inversely related to wavelength. At longer wavelengths no absorption occurs, because the energy is insufficient to excite electrons to transition across the energy gap between two bands. Above the bandgap energy, the shape of the absorption indicates whether the material has a direct or indirect bandgap. Consider the indirect and direct bandgap absorption curves in Fig. 5.4. The onset of absorption for a direct bandgap appears as a step, while that for an indirect bandgap is much more gradual. The shape of the absorption curve at energies higher than the bandgap is affected by the long-range order within the material. For this reason, the optical functions often indicate whether a material is amorphous, polycrystalline, or monocrystalline. Organic materials also exhibit absorption due to electronic transitions, but their band structure is related to molecular bonding [5].

The electronic transitions are the most commonly measured absorption phenomena, and their exact shape is related to the shape and symmetries of the energy bands. Therefore, they are represented by the largest variety of dispersion models. The Tauc-Lorentz (Sect. 5.3.7) and Cody-Lorentz (Sect. 5.3.8) describe the absorption of amorphous materials near their bandgap. The CPPB, Adachi, and

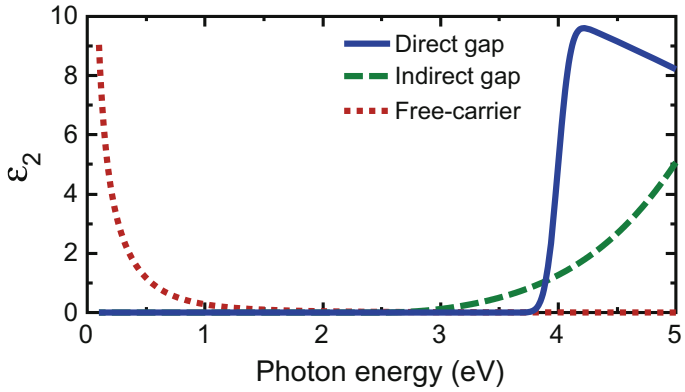

Fig. 5.4 Comparison between the ε_2 curves associated with direct and indirect interband transitions near the bandgap, along with intraband transitions associated with free carrier absorption

jhilfiker@jawoollam.com

PSEMI (Sect. 5.3.9) are useful for crystalline materials and direct bandgap transitions. For organic materials, it is more common to apply a sum of Gaussians (Sect. 5.3.6) or an empirical equation such as the b-spline (Sect. 5.3.10).

5.1.4.2 Conductivity or Free-Carriers

The second type of absorption we consider is that of free-carriers. This absorption occurs from electrons (or holes) which are no longer bound to an atom. Another way to consider this is that the electrons are already in the conduction band (holes in the valence band) and can absorb light to move within the band—in other words intraband transitions [6]. This is the common absorption mechanism for conductive materials such as metals and transparent conductive oxides (TCOs). They are generally modeled with some form of the Drude oscillator, described in Sect. 5.3.4. Figure 5.4 shows an example ε_2 spectra related to free-carrier absorptions. Unlike the electronic transitions, free carriers absorb more strongly as photon energy decreases, which corresponds to slower frequencies. As the frequency decreases, there is higher probability for energy transfer between the electromagnetic wave and the material.

5.1.4.3 Vibrational and Phonon Absorption

The final absorption mechanism we consider is due to interactions with molecular and lattice (phonon) vibrational modes. Because atoms are significantly heavier than electrons, the resonant frequencies of molecular vibrations are generally lower than electronic transition frequencies. Thus, this type of absorption primarily occurs at infrared (IR) wavelengths. The resonant frequency for a particular vibrational mode depends upon the mass and bond strengths of the atoms involved, as well as the molecular and lattice symmetry. Vibrational modes can be symmetric and antisymmetric, and include stretching, twisting and scissor motions, as illustrated in Fig. 5.5. Infrared light can only be absorbed by "infrared active" modes, which are modes with a pre-existing dipole moment because of ionic or polar bonds. As IR ellipsometry is not as common as UV, visible, and NIR ellipsometry, we will give

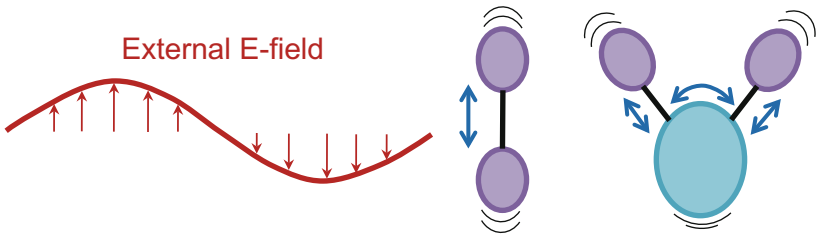

Fig. 5.5 Oscillating molecular vibrations can occur at slower frequencies such as used by Infrared SE

jhilfiker@jawoollam.com

less consideration to the dispersion equations for this region. The reader is directed to two excellent books on IR ellipsometry, one by Roseler [7] and another by Schubert [8]. However, we must point out that these infrared vibrational absorptions can alter the shape of ε_1 at NIR wavelengths through the Kramers-Kronig relationship and this influence can be modeled using a Sellmeier function (Sect. 5.3.1).

5.2 Representing the Dielectric Function

While a few dispersion equations are strictly empirical with no underlying physical basis, the majority incorporate the KK relations to connect the real and imaginary optical functions and maintain a physically plausible shape. In this section, we consider the general approach to describe the optical functions. We start by describing a resonance or absorption. Multiple absorptions are summed together to create the overall optical functions which describe contributions from different phenomena. Finally, we describe how to handle the contributions from absorptions outside the measured spectral range.

5.2.1 Representing Absorption Features

As described in Sect. 5.1, the dielectric function is strongly influenced by dipoles within a material. The form of the complex dielectric function that is described in Sect. 5.1.2 is a result of the strength of the dipole response combined with the level of energy loss near resonance. Most dispersion equations define the shape of ε_2 and then apply the KK integral relations to calculate ε_1. If we consider a single absorption (or resonance) as pictured in Fig. 5.3, the general shape of ε_2 can be described by the absorption amplitude, a broadening term, and the resonant energy (or frequency). Additional terms may be added to modify this basic shape depending on the type of dispersion model. Once the absorption shape is defined, the area under the ε_2 curve is integrated per (5.5a) to determine ε_1. Because of their resemblance to mechanical oscillators, these types of functions are often called "oscillator functions" or simply "oscillators". These functions will be seen time and again as we consider the actual dispersion equations in Sect. 5.3.

Most materials exhibit multiple absorptions, which occur at different energies, and the total optical function versus photon energy is the result of a combination of these phenomena. Figure 5.6 represents a material which has three different absorption phenomena occurring at different energies. Each can be described as a separate resonance and then summed together to describe the material's overall complex optical function. When comparing the three "oscillators" in Fig. 5.6, note that the narrower ε_2 absorptions are associated with a sharper dispersion feature in

jhilfiker@jawoollam.com

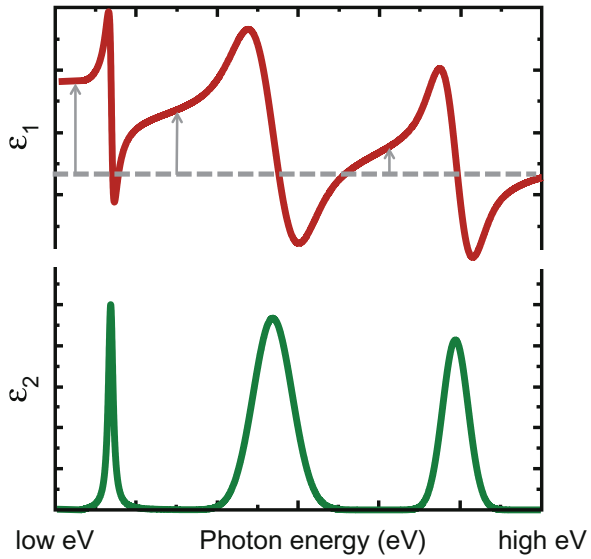

Fig. 5.6 Material dielectric function is influenced by absorption phenomena at different energies

ε_1. The dashed line and arrows illustrate how each resonant absorption increases the overall level of ε_1 as the incident light changes from higher to lower photon energies.

It is easy to visualize the absorption features as isolated resonant phenomena occurring at different energies. However, real materials are generally much more complex. The absorption phenomena, such as electronic transitions, can have multiple contributions and overlap to form the final shape of the material optical functions. Fortunately, many dispersion functions remain valid when summed together. This is shown in Fig. 5.7 for a CdTe material. The final shape consists of five individual dispersion equations, each contributing to the overall shape of ε_2.

When multiple absorptions overlap, it becomes difficult to connect the oscillator parameters—amplitude, broadening, etc.—to the physical origins of the absorption. Furthermore, in most cases more than one combination of oscillators can successfully describe the same dielectric function. If one of the primary goals of the measurement is to determine a material's complex optical function, it can be argued that any combination of oscillators that faithfully reproduces ε is acceptable. In these circumstances, an ad hoc combination of oscillators can be chosen to match

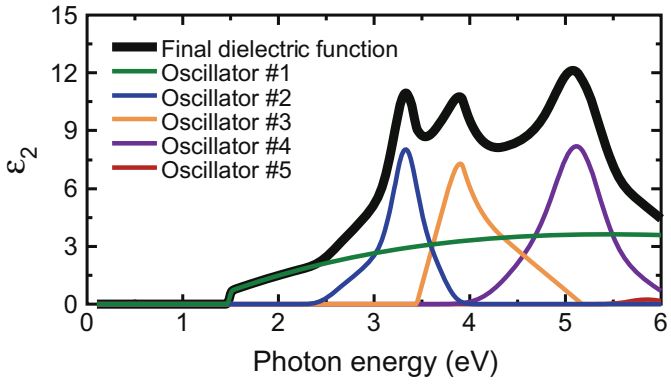

Fig. 5.7 Summation of multiple oscillators that "build-up" to give the overall shape of dielectric function (CdTe for the example)

jhilfiker@jawoollam.com

the overall shape of the function, and no attempt is made to tie oscillator parameters to specific physical properties such as bandgap energy, etc. The goal then is to create an optical function that is physical (i.e., fulfills the Kramer's Kronig relationship), and that best matches the measured SE data. It is also preferred that the optical function use a minimum number of free parameters while still accurately modeling the SE data.

5.2.2 *Absorptions Outside Measured Spectral Range*

SE measurements can only cover a limited range of energies, and this may be further limited during data analysis—restricting the final *investigated spectral range*. As mentioned earlier, the shape of the optical functions are influenced by their values at all energies. Thus, we need to consider what occurs outside the investigated spectral range. As a simple example, consider a material that is transparent throughout the investigated spectral range. While transparent, ε_1 still increases toward higher energies; that is, it must maintain normal dispersion. As discussed earlier, normal dispersion is the result of the contribution of the oscillating dipoles to the polarization field as the photon energy approaches their resonant energy. Thus, it is the resonance at higher photon energies that causes ε_1 to increase at shorter wavelengths (higher photon energies). The Sellmeier equation approximates normal dispersion by placing a resonance at higher photon energy outside the investigated spectral range.

Even when absorption occurs within the investigated spectral range, the overall ε_1 shape is altered by any absorption at higher or lower photon energies. This is shown in Fig. 5.8 where three ε_2 absorption phenomena occur between 1 and 6 eV. Our measured photon energies only access the middle absorption. If we were to describe only this middle ε_2 absorption, the KK integration would produce the dashed ε_1 curve in Fig. 5.8. However, this ε_1 would not match our experimental SE data, since it does not retain the influence of the absorptions outside the measured energy range. The correct ε_1 shape is shown by the solid curve, because it includes contributions from the out-of-range absorptions. Comparing the solid and dashed curves, the primary difference is an offset and upward tilt to the general ε_1 shape at higher photon energies. We can raise the ε_1 curve by adding an offset, often called $\varepsilon_1(\infty)$. The offset accounts for absorptions that are well beyond the investigated spectral range. If absorptions occur close to our investigated spectral range, they may also "tilt" the ε_1 curve. This effect can be modeled by using "poles" (Sect. 5.3.1). A pole alters ε_1 in the same manner as an absorption that is located outside the investigated spectral range, without describing the actual shape of that absorption. A pole placed at higher photon energies both raises and tilts the ε_1 curve upward toward high energies (shorter wavelengths). A pole placed at lower energies will lower and tip the ε_1 curve downward as it extends toward lower photon

jhilfiker@jawoollam.com

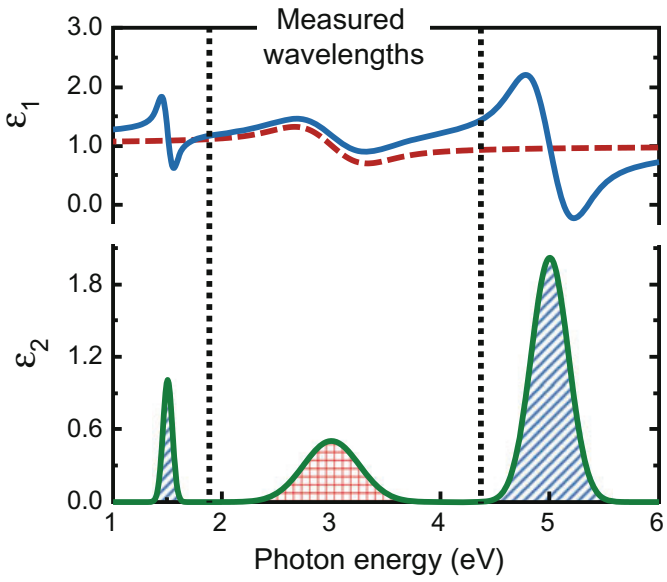

Fig. 5.8 Three absorptions are shown, but only the center peak is within the measured wavelength range. A KK integral from this center absorption (hatched area) would produce the dashed ε_1 curve shown above. However, the absorptions outside the measured spectral range still affect the shape of ε_1 as shown in the solid ε_1 curve which is calculated by the KK integral under all three ε_2 features

energies (longer wavelengths). Thus, the effect on ε_1 from absorptions that are external to the investigated spectral range can be approximated using high and low energy poles, along with an offset—$\varepsilon_1(\infty)$.

5.3 Common Dispersion Relations

We will now review some dispersion relations that are commonly used to describe photovoltaic materials. For each relation, we provide the underlying equations, describe their general shape, and list the free parameters used to modify the shape during data analysis. We also discuss the merits and limitations of each equation and mention common applications. For each equation, a table is provided so that the reader can conveniently locate pertinent information.

While the equations are discussed individually, most can be added together to describe more complex dispersion shapes. For example, the complex dielectric function may be represented by a linear summation of terms, such as:

$$\varepsilon = \varepsilon_1 - i\varepsilon_2 = \varepsilon_1(\infty) + \text{Sellmeier}(A_1, E_1) + \text{Lorentz}(A_2, E_{02}, \Gamma_2) + \text{Gaussian}(A_3, E_{03}, \Gamma_3) \tag{5.6}$$

Each absorption or resonance feature in ε_2 is represented by a corresponding "oscillator" equation and the corresponding variables. In many cases, the real part, ε_1, of an oscillator is derived using Kramers-Kronig integral relationship. The real part, ε_1, is often supplemented by one or two Sellmeier terms and the constant offset, denoted $\varepsilon_1(\infty)$. Note that these only affect ε_1, and they account for any high-frequency resonances which are not already considered by the listed equations.

jhilfiker@jawoollam.com

While many of the individual equations have an offset equal to +1, this can be replaced by the variable offset of $\varepsilon_1(\infty)$ to add more flexibility to the final dielectric function shape.

5.3.1 Sellmeier

The Sellmeier dispersion [9] function models a material as a collection of oscillating dipoles, which resonate at a specific energy (frequency or wavelength) as discussed in Sect. 5.1.2. Sellmeier theory assumes that the oscillating dipoles have no absorption, so the oscillators have zero broadening and the resulting equations can be written as:

$$\varepsilon_1(\lambda) = 1 + \frac{A\,\lambda^2}{\lambda^2 - \lambda_0^2} \tag{5.7}$$

or equivalently,

$$\varepsilon_1(E) = 1 + \frac{A\,E_0^2}{E_0^2 - E^2} \tag{5.8}$$

where there are two free parameters for each Sellmeier term: amplitude A, and a resonant wavelength λ_0 or resonant energy E_0. Alternative Sellmeier expressions exist with different numerator terms. This will be discussed in Sect. 5.3.3 for the corresponding Lorentz equations. A very simplified Sellmeier expression, referred to as a *Pole* is given as:

$$\varepsilon_1(E) = 1 + \frac{A}{E_0^2 - E^2} \tag{5.9}$$

Because there is no broadening term, the Sellmeier and Pole equations are purely real ($\varepsilon_2 = 0$) and each term approaches $+\infty$ or $-\infty$ at the resonant condition. This is demonstrated in Fig. 5.9 for a single Sellmeier term per (5.7) with $\lambda_0 = 200$ nm. With this single Sellmeier term, ε_1 approaches +1 at short wavelengths (large E) and approaches $1 + A$ at long wavelengths (small E).

The Sellmeier equations are used to describe transparent materials that exhibit normal dispersion within the investigated spectral range. The resonant frequency is generally located at UV wavelengths, beyond the shortest wavelength of the investigated spectral range. Multiple Sellmeier terms can be summed to represent the effect from multiple resonances, as:

jhilfiker@jawoollam.com

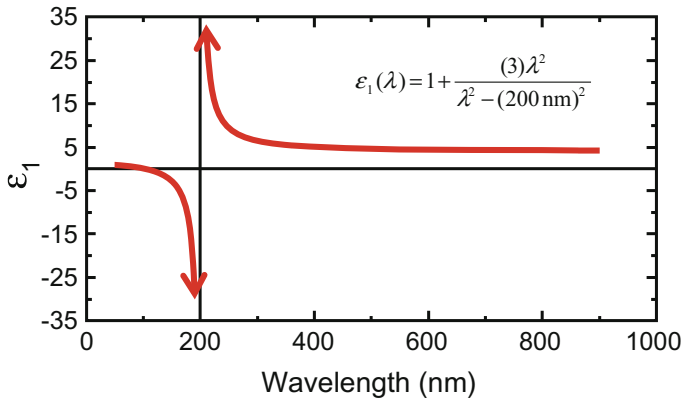

Fig. 5.9 Sellmeier dispersion shown for (5.7) with amplitude equal to 3 and resonant wavelength set to 200 nm

$$\varepsilon_1(\lambda) = \varepsilon_1(\infty) + \sum_j \frac{A_j \lambda^2}{\lambda^2 - \lambda_{0j}^2} \tag{5.10}$$

or

$$\varepsilon_1(E) = \varepsilon_1(\infty) + \sum_j \frac{A_j E_0^2}{E_{0j}^2 - E^2} \tag{5.11}$$

The variable offset, $\varepsilon_1(\infty)$, has been added to accommodate additional resonances well outside the investigated spectral range, because an offset other than +1 may be required to accomplish the desired effect of raising or lowering ε_1. It is common practice to use two Sellmeier terms where a UV term describes the higher energy electronic transitions while an IR term describes molecular vibrations at lower energy. The UV term tips ε_1 upward toward short wavelengths, while the IR term tips ε_1 down toward longer wavelengths and is only needed for materials with strong IR resonance. There is less sensitivity to the IR term unless the investigated spectral range extends well into the infrared. For this reason, it is common to fix the resonant energy of the IR term at a nominal value (e.g. 0.001 eV) and only fit the IR amplitude, which helps reduce correlation by decreasing the total number of variable parameters.

There are several commonly seen forms of the Sellmeier function. One is used in the data sheets supplied with Schott glass, where (5.10) is rewritten in the following form [10]:

$$n^2(\lambda) - 1 = \frac{B_1 \lambda^2}{(\lambda^2 - C_1)} + \frac{B_2 \lambda^2}{(\lambda^2 - C_2)} + \frac{B_3 \lambda^2}{(\lambda^2 - C_3)} \tag{5.12}$$

Note that the C parameters are the *square* of the resonant wavelengths. Another form of the Sellmeier explicitly defines the term $-C\lambda^2$, which curves the optical function downward at longer wavelengths [11]:

jhilfiker@jawoollam.com

Table 5.1 Details of the Sellmeier equation

Sellmeier equation	
# of free parameters	2 or 3 with $\varepsilon_1(\infty)$
for $\varepsilon_{2:}$	0
for $\varepsilon_{1:}$	2–3 [A, E_0] or [A, λ_0] with $\varepsilon_1(\infty)$ optional
Primary applications:	Transparent spectrum of dielectrics and organics

$$n^2(\lambda) = \varepsilon_1(\infty) + \frac{A\lambda^2}{\lambda^2 - B^2} - C\lambda^2 \tag{5.13}$$

This is equivalent to a two-term version of (5.10), where the resonant wavelength of the second term, λ_{02}, is set to a very large, finite value.

The Sellmeier model works well in spectral regions where there is no absorption. It provides a physically plausible normal dispersion shape with the amplitude and curvature needed for ε_1 by varying the two adjustable parameters, amplitude and resonant frequency. However, the relationship between the adjustable parameters and the final shape is not as intuitive as the Cauchy equation (Sect. 5.3.2). In addition, care must be taken to avoid placing the resonant condition within the investigated spectral range to avoid the large singularity which occurs, as shown near $\lambda = 200$ nm in Fig. 5.9. Table 5.1 provides an overview of the Sellmeier equation.

5.3.2 *Cauchy*

The Cauchy is actually an empirical model that predates the Sellmeier equation. However, it can be derived as a binomial series expansion of a single Sellmeier term. The Cauchy function [12] is written as:

$$n(\lambda) = A + \frac{B}{\lambda^2} + \frac{C}{\lambda^4} + \ \ldots \tag{5.14a}$$

$$k(\lambda) = 0 \tag{5.14b}$$

The simplicity of the Cauchy equation makes it very convenient and it is the most widely-used model for transparent materials. The Cauchy equation is also intuitive to use: A sets the amplitude of the index while B and C add curvature to produce normal dispersion. When wavelength is limited to a small range, two terms (A and B) are often adequate. The C term helps to define the index curvature over a broader wavelength range. With wavelength units in microns, the typical range for B and C is from +0.001 to +0.05 and −0.001 to +0.005, respectively.

The Cauchy is only accurate when $n(\lambda)$ follows normal dispersion. The standard 3-term Cauchy does not have a mechanism to produce downward tip of the index at

jhilfiker@jawoollam.com

NIR wavelengths caused by an IR resonance. However, the Cauchy equation can be modified to the following form:

$$n(\lambda) = A + \frac{B}{\lambda^2} + \frac{C}{\lambda^4} - D\lambda^2 \tag{5.15}$$

where D allows a downward tip at long wavelengths. The "$D\lambda^2$" term is equivalent to the last term of the Sellmeier function in (5.13). The downward tip is demonstrated in Fig. 5.10, which compares a 3-term Cauchy (5.14a), a 4-term modified Cauchy (5.15) and a sum of two-term Sellmeier [Pole form, (5.9)]. In this case, the Sellmeier is still generally preferred as it reduces the total number of free-parameters because the IR resonant energy was fixed at a nominal value.

The Cauchy equation can also be extended to handle the onset of absorption by replacing (5.14b) with Urbach absorption [13]:

$$k(E) = \alpha e^{\beta(E - E_b)} \tag{5.16}$$

The Urbach equation represents a small exponentially decaying absorption below the bandgap of many amorphous materials. The extinction coefficient is described by an amplitude α, an exponent factor β, and the band-edge energy E_b. The Urbach absorption is only accurate when the exponential absorption is sufficiently small ($k < 0.01$) such that the index does not exhibit anomalous dispersion.

The main drawback of the Cauchy equation is that it can create physically implausible shapes that defy normal dispersion if either B or C is a strong negative value. It is advisable to always view a plot of the final index dispersion after data fitting is completed. If the index decreases toward short wavelengths, it defies normal dispersion and calls into question the resulting model. This often indicates the model is still missing some important detail, such as roughness, index gradient or even absorption.

The Cauchy and Sellmeier relations are used to model a wide variety of dielectrics and organics. The main constraint for both is that they can only be applied to a spectral range where the material is transparent. The Sellmeier is

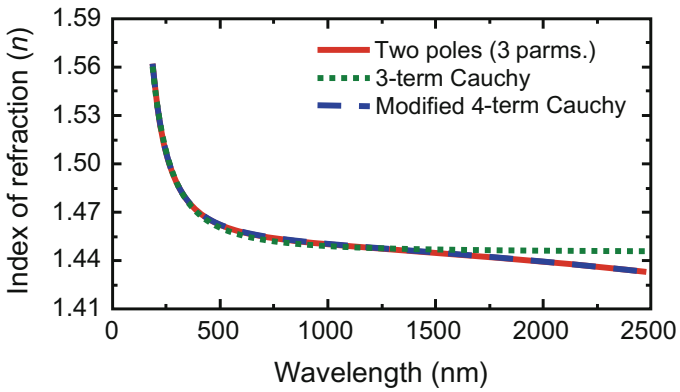

Fig. 5.10 Index of fused silica described using a 3-term Cauchy, a 4-term Cauchy, and a sum of two Sellmeier terms. The standard 3-term Cauchy index remains flat in the NIR while the IR Sellmeier relation and the 4th term of the Cauchy can provide the downward index tip due to IR resonance

jhilfiker@jawoollam.com

Table 5.2 Details of the standard 3-term Cauchy equation

3-term Cauchy equation	
# of free parameters	3
for $\varepsilon_{2:}$	0
for $\varepsilon_{1:}$	3 [A, B, C]
Primary applications:	Transparent spectrum of dielectrics and organics

preferred if the investigated spectral range extends far enough into the NIR such that the index begins to tilt downward due to strong IR phonon resonances (such as with SiO_2) or in response to IR absorption from free-carriers (such as with SnO_2:F). If absorption extends into the investigated spectral range, then neither the Cauchy nor Sellmeier will be adequate. In the following sections, we cover a variety of models which describe absorbing optical functions. Table 5.2 provides an overview of the Cauchy equation.

5.3.3 *Lorentz*

The Lorentz oscillator model assumes that the response of electrons to the oscillating electric field is similar to the response of a harmonically driven mass on a spring subject to a dissipative force. In this analogy, the mass corresponds to the electron cloud, the spring represents the electrostatic forces on the electron cloud due to all other electrons and nuclei in the solid, and the dissipative force (friction for the mass on a spring) represents the energy loss due to emission of a photon [14]. This model is classical in that the electrons may possess any amount of kinetic energy as opposed to the allowed energy levels and bands of quantum theory. The Lorentz oscillator model is generally formulated as:

$$\varepsilon(E) = \varepsilon_1(E) - i\varepsilon_2(E) = 1 + \frac{A}{E_0^2 - E^2 + i\Gamma E} \tag{5.17}$$

Each oscillator is described by three parameters: the oscillator strength A, center energy E_0, and broadening Γ. The Lorentz (5.17) reduces to the Pole of (5.9) when $\Gamma = 0$. The broadening term, Γ, can be visualized as the full width of ε_2 at half its maximum value (FWHM). When Γ is small, the region of anomalous dispersion extends approximately $\pm\Gamma/2$ around E_0 as shown in Fig. 5.11.

The Lorentz equation can also be constructed with different choice of numerator, as in:

$$\varepsilon(E) = \varepsilon_1(E) - i\varepsilon_2(E) = \varepsilon_1(\infty) + \frac{A\,\Gamma\,E_0}{E_0^2 - E^2 + i\Gamma E} \tag{5.18}$$

jhilfiker@jawoollam.com

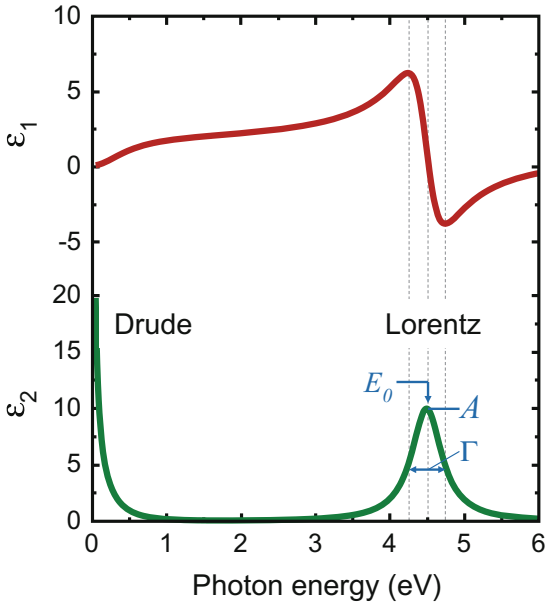

Fig. 5.11 The complex dielectric function associated with a Drude and a Lorentz oscillator function

$$\varepsilon(E) = \varepsilon_1(E) - i\varepsilon_2(E) = \varepsilon_1(\infty) + \frac{A\,E_0}{E_0^2 - E^2 + i\Gamma E} \tag{5.19}$$

or

$$\varepsilon(E) = \varepsilon_1(E) - i\varepsilon_2(E) = \varepsilon_1(\infty) + \frac{A\,E_0^2}{E_0^2 - E^2 + i\Gamma E} \tag{5.20}$$

These three equations provides a similar ε_2 shape, but with different meanings for A. In (5.18), A is the height of ε_2 at the center energy E_0. For (5.19), A is proportional to the area under the ε_2 curve and the ε_2 value at E_0 equals A/Γ. For (5.20), A is equivalent to the difference between ε_1 at energies significantly higher and lower than the oscillator's center energy. Interestingly, for each of these Lorentz equations, the actual peak in ε_2 shifts to energies below E_0 as Γ increases.

A Lorentz oscillator of the form from (5.18) is shown in Fig. 5.11. The oscillator resonance is at 4.5 eV with amplitude $A = 10$ and broadening $\Gamma = 1$ eV. Note the near-symmetric shape of the absorption and the relatively long tails extending on each side of the resonant absorption before ε_2 nears zero. For this reason, the Lorentz oscillator is seldom used to model dielectrics or semiconductors which require a transparent spectral region. Rather, the Lorentz model is useful for metals which remain absorbing across the entire spectrum. The Lorentz (5.17) also reduces to the Drude function (Sect. 5.3.4) as E_0 approaches zero energy, which is very useful for describing the free electron absorption that occurs in transparent conducting oxides and heavily doped semiconductors. Table 5.3 provides an overview of the Lorentz oscillator equation.

jhilfiker@jawoollam.com

Table 5.3 Details of the Lorentz oscillator equation

Lorentz oscillator equation	
# of free parameters	4
for $\varepsilon_{2:}$	3 [A, E_0, Γ]
for $\varepsilon_{1:}$	1 [$\varepsilon_1(\infty)$]
Primary applications:	Metals and other absorbing materials

5.3.4 Drude

The Drude model [15] is a classical kinetic model of conductivity (1/resistivity) that was developed by Drude and Sommerfeld in the late 1800's. It describes the interaction of time-varying electric fields with *free carriers*—electrons or "holes" [15]—which move freely in conductive materials.

The form of the Drude oscillator is that of a Lorentz oscillator (5.17) with zero center energy (no restoring force):

$$\varepsilon(E) = \varepsilon_1(E) - i\varepsilon_2(E) = \varepsilon_1(\infty) - \frac{A}{E^2 - i\Gamma E} \tag{5.21}$$

where the quantity $\varepsilon_1(\infty)$ is the high-frequency dielectric constant and the two free parameters are amplitude, A, and broadening, Γ. Interestingly, the Drude equation can also be written such that the free parameters are the optical resistivity ρ_{opt} (units are Ω-cm), and the mean scattering time τ (units are seconds) [16]:

$$\varepsilon(E) = \varepsilon_1(E) - i\varepsilon_2(E) = \varepsilon_1(\infty) - \frac{\hbar^2}{\varepsilon_0 \rho_{\text{opt}}(\tau \cdot E^2 - i\hbar E)} \tag{5.22}$$

where $\hbar$ is the reduced Plank's constant ($\sim 6.582 \times 10^{-16}$ eV · s) and ε_0 is the vacuum dielectric constant ($\sim 8.854 \times 10^{-14}$ s/Ω-cm). Related parameters of interest include the carrier effective mass m^*, the optical carrier concentration N_{opt}, and the optical carrier mobility μ_{opt}, which are related to optical resistivity by:

$$\rho_{\text{opt}} = \frac{m^*}{N_{\text{opt}} q^2 \tau} = \frac{1}{q \mu_{\text{opt}} N_{\text{opt}}} \tag{5.23}$$

where q is the single electron charge equal to 1.6×10^{-19} C.

Regardless which equation is chose, the Drude has two free parameters to describe a shape with increasing absorption toward lower frequencies (lower E, longer λ) as shown in Fig. 5.11. The primary application of the Drude oscillator is to describe the free-carrier absorption prevalent in metals, heavily-doped semiconductors, and transparent conductive oxides. Table 5.4 provides an overview of the Drude oscillator equation. For a material such as indium tin oxide (ITO), it is common to use the Drude oscillator to describe the free-carrier absorption and then

jhilfiker@jawoollam.com

Table 5.4 Details of the Drude oscillator equation

Drude equation	
# of free parameters	3
for $\varepsilon_{2:}$	2 [A, Γ] or [ρ_{opt}, τ] or [N_{opt}, μ_{opt}]
for $\varepsilon_{1:}$	1 [$\varepsilon_1(\infty)$]
Primary applications:	Metals, heavily-doped semiconductors, and transparent conductive oxides (TCOs)

supplement the short-wavelength shape with Tauc-Lorentz or Gaussian equations to describe the effects of electronic transitions. We describe these additional dispersion equations next.

5.3.5 Harmonic Oscillator Approximation

The classic Harmonic oscillator model is very similar to the Lorentz oscillator, but is derived from quantum mechanical perturbation theory:

$$\varepsilon(E) = \varepsilon_1(E) - i\varepsilon_2(E) = 1 + \frac{A}{E + E_0 - i\gamma} - \frac{A}{E - E_0 - i\gamma} \tag{5.24}$$

which can be rearranged as:

$$\varepsilon(E) = \varepsilon_1(E) - i\varepsilon_2(E) = 1 + \frac{2AE_0}{E_0^2 - E^2 + i2\gamma E + \gamma^2} \tag{5.25}$$

If we substitute $\Gamma = 2\gamma$ and then multiply the numerator by Γ, we can rewrite the Harmonic oscillator as:

$$\varepsilon(E) = \varepsilon_1(E) - i\varepsilon_2(E) = \varepsilon_1(\infty) + \frac{A\Gamma E_0}{E_0^2 - E^2 + i\Gamma E + \frac{1}{4}\Gamma^2} \tag{5.26}$$

such that amplitude, A, is approximately the peak of ε_2 at the resonant energy and Γ is approximately the FWHM value found with the Lorentz oscillator. Equation (5.26) is nearly identical to the corresponding Lorentz oscillator of (5.18), except for the $\frac{1}{4}\Gamma^2$ term in the denominator. Interestingly, the energy position for the ε_2 peak of the Harmonic oscillator is less sensitive to the broadening term and shifts slightly to higher photon energies rather than to lower photon energies like with the Lorentz oscillator behavior.

The Lorentz and Harmonic oscillator shapes are compared in Fig. 5.12. The two oscillators appear different if the same parameters are used for A, E_0, and Γ. However, this is a result of the $\frac{1}{4}\Gamma^2$ term in the denominator. A simple adjustment

jhilfiker@jawoollam.com

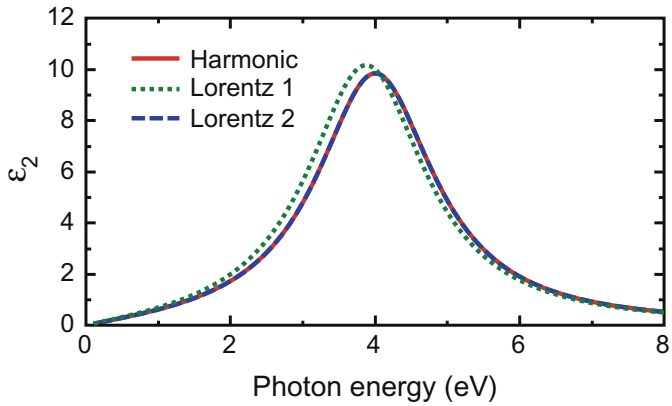

Fig. 5.12 Comparison of a harmonic oscillator [(5.25): $A = 10$ eV, $E_0 = 4$ eV, $\Gamma = 2$ eV] with two Lorentz oscillators (5.17). The first Lorentz has the same parameter values as the harmonic and it has a noticeable peak shift to lower photon energies with increased amplitude. The second Lorentz has parameters ($A = 9.7014$ eV, $E_0 = 4.1231$ eV, $\Gamma = 2$ eV) adjusted to match the harmonic shape

of Lorentz oscillator parameters, $E_{0-\mathrm{Lor}} = \sqrt{E_{0-\mathrm{Har}}^2 + \frac{1}{4}\Gamma^2}$ and $A_{\mathrm{Lor}} = A_{\mathrm{Har}} \cdot E_{0-\mathrm{Har}} / \sqrt{E_{0-\mathrm{Har}}^2 + \frac{1}{4}\Gamma^2}$, allows the Lorentz to perfectly match the Harmonic. Thus, when fitting measured SE data, the Harmonic and Lorentz oscillators can produce equivalent shapes and can be used interchangeably; however, the center energies and amplitudes will generally be different.

Based on its origin, the harmonic oscillator is often used to describe semiconductor electronic transitions. While the shape can adequately describe the absorption very close to a critical point energy, it requires many extra oscillators that have no intrinsic physical meaning in order to match the background spectral dispersion effectively. If the data extend below the bandgap of the material, the Harmonic oscillator will extend too much beyond the transparent region to be effective. For this reason, the Harmonic oscillator is reserved for absorbing materials and relegated to the same applications of the Lorentz oscillator. Table 5.5 provides an overview of the Harmonic oscillator equation. In the following sections, we describe dispersion equations which can be used with both an absorbing and a transparent region (Gaussian, Tauc-Lorentz, and Cody-Lorentz).

Table 5.5 Details for the harmonic oscillator equation

Harmonic oscillator equation	
# of free parameters	4
for $\varepsilon_{2:}$	3 [A, E_0, Γ]
for $\varepsilon_{1:}$	1 [$\varepsilon_1(\infty)$]
Primary applications:	Metals and other absorbing materials

jhilfiker@jawoollam.com

5.3.6 Gaussian

The main drawback of the Lorentz and Harmonic oscillators is the long ε_2 tail outside of the central absorption spectrum defined as the following region surrounding the center energy:

$$E - \frac{\Gamma}{2} < E_0 < E + \frac{\Gamma}{2} \tag{5.27}$$

This often leads to unwanted absorption extending into spectral regions where the material should be transparent. One alternative is to replace the Lorentz shape with a Gaussian line shape to describe ε_2 as [17, 18]:

$$\varepsilon_2(E) = Ae^{-\left(\frac{E-E_0}{\sigma}\right)^2} - Ae^{-\left(\frac{E+E_0}{\sigma}\right)^2} \tag{5.28}$$

where our free parameters are amplitude A, center energy E_0, and broadening σ. We can modify the equation with

$$\sigma = \frac{\Gamma}{2\sqrt{\ln(2)}} \tag{5.29}$$

to define the broadening, Γ, with respect to the FWHM value and approximate the region of anomalous dispersion per (5.27). The form of (5.28) defines a Gaussian at both positive and negative frequencies to maintain the odd symmetry for ε_2, as required by Kramers-Kronig criteria [specifically (5.30b)]:

$$\varepsilon_1(-E) = \varepsilon_1(E) \tag{5.30a}$$

and

$$\varepsilon_2(-E) = -\varepsilon_2(E) \tag{5.30b}$$

such that the real part, ε_1, can be effectively calculated from the Kramers-Kronig relation (5.5a).

Just like the Lorentz, there are three free parameters to describe the ε_2 absorption shape: amplitude A, broadening Γ, and center energy E_0. Figure 5.13 compares the dielectric functions of a Gaussian to a Lorentz oscillator. The ε_2 for the Gaussian oscillator approaches zero much more rapidly than the Lorentz outside the central absorption region. The absorption shapes for both Lorentz and Gaussian remain roughly symmetric about the resonant condition.

In real materials, the absorption is seldom this symmetric and contributions from more than one absorption phenomena require combination of more than one Lorentz or Gaussian to match the material's optical functions. It is very common to use

jhilfiker@jawoollam.com

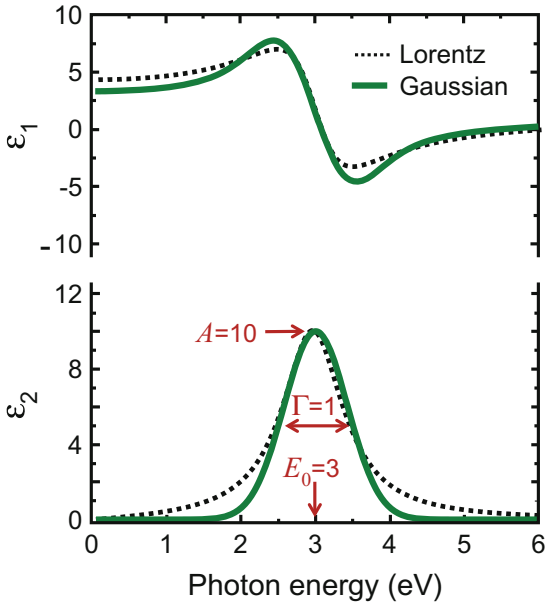

Fig. 5.13 Shape of Gaussian with parameters, possible with Lorentz for comparison

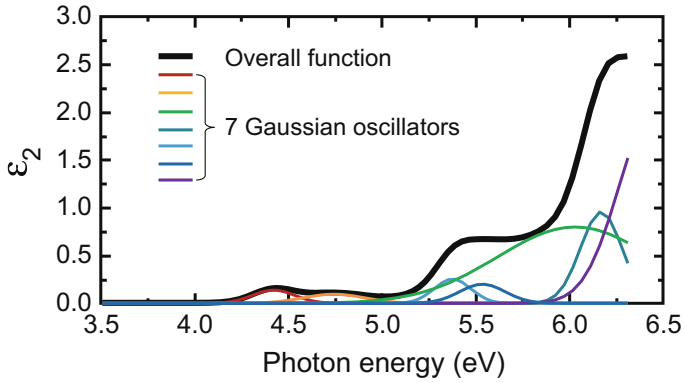

Fig. 5.14 The ε_2 spectra for an organic photoresist composed of seven individual Gaussian oscillators

several Gaussian oscillators to describe the dielectric function of organic films. For example, the ε_2 spectrum for an organic photoresist material is shown in Fig. 5.14. The overall ε_2 function results from the summation of seven individual Gaussian oscillators, which are also shown. Another common application of Gaussian oscillators is to supplement other dispersion functions when describing the electronic transitions of dielectrics and semiconductors. Table 5.6 provides an overview of the Gaussian oscillator equation.

Table 5.6 Quick details for the Gaussian oscillator equation

Gaussian oscillator equation	
# of free parameters	4
for $\varepsilon_{2:}$	3 [A, E_0, Γ]
for $\varepsilon_{1:}$	1 [$\varepsilon_1(\infty)$]
Primary applications:	Organics, dielectrics, and semiconductors

jhilfiker@jawoollam.com

5.3.7 Tauc-Lorentz

The Tauc-Lorentz model was developed by Jellison and Modine [19] to provide a dispersion equation which only absorbs light above the material bandgap. It models the dielectric function of many amorphous materials particularly well. Close to the band edge, the absorption of the Tauc-Lorentz equation follows a Tauc law formula:

$$\varepsilon_2(E) \propto \frac{\left(E - E_g\right)^2}{E^2} \tag{5.31}$$

The absorption from the Tauc-Lorentz is separated into two regions:

$$\varepsilon_2(E) = \frac{AE_0C\left(E - E_g\right)^2}{\left(E^2 - E_0^2\right)^2 + C^2E^2} \cdot \frac{1}{E} \quad E > E_g \tag{5.32a}$$

$$\varepsilon_2(E) = 0 \quad E \le E_g \tag{5.32b}$$

Using the KK integral [(5.5a), but repeated here for convenience]:

$$\varepsilon_1(E) = \varepsilon_1(\infty) + \frac{2}{\pi} P \int_{E_g}^{\infty} \frac{E' \varepsilon_2(E')}{E'^2 - E^2} \mathrm{d}E' \tag{5.33}$$

where the integration need consider only energies above the bandgap, as $\varepsilon_2 = 0$ for energies less than E_g. Jellison and Modine provide the closed form solution for ε_1 [19, *specifically the erratum*]:

$$\begin{aligned}\varepsilon_1(E) = \varepsilon_1(\infty) &+ \frac{A\,C}{\pi\zeta^4} \cdot \frac{a_{\ln}}{2\alpha E_0} \ln\left(\frac{E_0^2 + E_g^2 + \alpha E_g}{E_0^2 + E_g^2 - \alpha E_g}\right) - \frac{A}{\pi\zeta^4} \cdot \frac{a_{\text{atan}}}{E_0}\left[\pi - \text{atan}\left(\frac{2E_g + \alpha}{C}\right) + \text{atan}\left(\frac{-2E_g + \alpha}{C}\right)\right] \\ &+ 2\frac{A\,E_0}{\pi\zeta^4\alpha} E_g\left(E^2 - \gamma^2\right)\left[\pi + 2\,\text{atan}\left(2\frac{\gamma^2 - E_g^2}{\alpha C}\right)\right] - \frac{A\,E_0\,C}{\pi\zeta^4} \cdot \frac{E^2 + E_g^2}{E} \ln\left(\frac{\left|E - E_g\right|}{E + E_g}\right) \\ &+ 2\frac{A\,E_0\,C}{\pi\zeta^4} E_g \ln\left(\frac{\left|E - E_g\right| \cdot \left(E + E_g\right)}{\sqrt{\left(E_0^2 - E_g^2\right)^2 + E_g^2C^2}}\right)\end{aligned} \tag{5.34}$$

with

$$a_{\ln} = \left(E_g^2 - E_0^2\right)E^2 + E_g^2C^2 - E_0^2\left(E_0^2 + 3E_g^2\right) \tag{5.35a}$$

jhilfiker@jawoollam.com

$$a_{\text{atan}} = \left(E^2 - E_0^2\right)\left(E_0^2 + E_g^2\right) + E_g^2 C^2 \tag{5.35b}$$

$$\zeta^4 = \left(E^2 - \gamma^2\right)^2 + \frac{\alpha^2 C^2}{4} \tag{5.35c}$$

$$\alpha = \sqrt{4E_0^2 - C^2} \tag{5.35d}$$

$$\gamma = \sqrt{E_0^2 - \frac{C^2}{2}} \tag{5.35e}$$

While these equations are quite intimidating, a close inspection shows that only five free parameters describe the dielectric function: amplitude A, resonant energy E_0, broadening C, bandgap energy E_g, and $\varepsilon_1(\infty)$. Unlike the Lorentz, Harmonic, and Gaussian, the Tauc-Lorentz produces a more asymmetric ε_2 shape. A Tauc-Lorentz with optical functions matching those of an amorphous silicon film is shown in Fig. 5.15 with $A = 124$, $E_0 = 3.44$ eV, $C = 2.52$ eV and $E_g = 1.2$ eV. Looking closely at the Tauc-Lorentz shape, the energy where ε_2 reaches a peak will shift to values above E_0 as the broadening increases.

The Tauc-Lorentz provides a more realistic representation of real-world materials and is widely used to describe many amorphous dielectrics and semiconductors. Most importantly, it remains transparent below the bandgap of the material. Table 5.7 provides an overview of the Tauc-Lorentz equation.

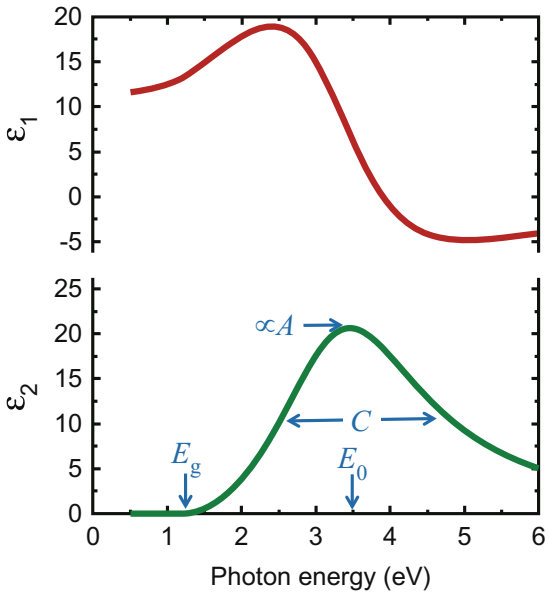

Fig. 5.15 Tauc-Lorentz with parameters matched to the shape of the optical functions for a-Si:H

jhilfiker@jawoollam.com

Table 5.7 Details of the Tauc-Lorentz equation

Tauc-Lorentz equation	
# of free parameters	5
for $\varepsilon_{2:}$	4 [A, E_0, C, E_g]
for $\varepsilon_{1:}$	1 [$\varepsilon_1(\infty)$]
Primary applications:	Amorphous semiconductors and dielectrics

5.3.8 Cody-Lorentz

The Cody-Lorentz function, developed by Ferlauto et al. [20] was designed to model amorphous materials, just like the Tauc-Lorentz. It is similar to the Tauc-Lorentz in that it defines the bandgap energy E_g and a Lorentzian absorption peak (parameters A, E_0, and Γ). However, the two models behave differently in the absorption-onset at photon energies slightly greater than E_g. In that region, the Tauc-Lorentz follows a Tauc law formula (5.31) while the Cody-Lorentz assumes:

$$\varepsilon_2(E) \propto \left(E - E_g\right)^2 \tag{5.36}$$

The Cody-Lorentz also includes an Urbach absorption term for the small absorptions that may occur below the bandgap. The ε_2 portion of the Cody-Lorentz oscillator model is separated into two energy regions and given as:

$$\varepsilon_2(E) = \frac{E_1}{E}\exp\left(\frac{E - E_t}{E_u}\right) \quad 0 < E \le E_t \tag{5.37a}$$

$$\varepsilon_2(E) = G(E)L(E) = \left[\frac{\left(E - E_g\right)^2}{\left(E - E_g\right)^2 + E_p^2}\right]\left[\frac{AE_0\Gamma E}{\left(E^2 - E_0^2\right)^2 + \Gamma^2 E^2}\right] \quad E > E_t \tag{5.37b}$$

where

$$E_1 = E_t G(E_t) L(E_t) \tag{5.37c}$$

The KK integration must now be split into multiple terms to cover integration of the Urbach and the Lorentz contributions as:

$$\varepsilon_1(E) = \varepsilon_1(\infty) + \frac{2E_1}{\pi} P \int_0^{E_t} \frac{\exp\left[\left(E' - E_t\right)/E_u\right]}{E'^2 - E^2} dE' + \frac{2}{\pi} P \int_{E_t}^{\infty} \frac{E' G(E') L(E')}{E'^2 - E^2} dE' \tag{5.38}$$

jhilfiker@jawoollam.com

In the equation above, E_t is the separation between the Urbach tail transitions and the band-to-band transitions. In the above equations, Ferlauto defines E_t as an absolute energy. In commercial software (WVASE®, for example), E_t is defined as an offset from the bandgap energy:

$$E_t = E_t^{\text{Ferlauto}} - E_g \tag{5.39}$$

The G(E) and L(E) functions define the Cody absorption behavior and the Lorentz oscillator function, respectively. The parameter E_p allows the user to define the energy, $E_g + E_p$, where the function transitions from a Cody absorption behavior (5.36) to the Lorentzian absorption.

Unlike the *Cauchy* model, this Urbach absorption tail is fully Kramer-Kronig consistent—that is, the exponential Urbach absorption in $\varepsilon_2(E)$ has a Kramers-Kronig transformed counterpart in $\varepsilon_1(E)$. The internal parameter E_1 guarantees that the ε_2 function transitions smoothly at E_t. The quantity E_1/E guarantees that the Urbach exponential function exactly matches $G(E)L(E)$ at E_t. The quantity E_u defines the exponential rate of decay; specifically where the Urbach absorption equal e^{-1} of its maximum value of E_1/E.

In the absence of the Urbach absorption tail, the Cody-Lorentz shape is very similar to the Tauc-Lorentz, with slight difference in how the absorption increases near the bandgap. The primary Cody-Lorentz parameters of interest become A, E_0, C, E_g, and E_p. This leads to slightly improved fits to amorphous semiconductor data with only a single extra parameter compared to the Tauc-Lorentz.

Standard SE measurements are generally insensitive to the low absorption values described by the Urbach tail (see log-scale plot of Fig. 5.16). Thus, it is most practical to use the Cody-Lorentz without the Urbach absorption. To set $\varepsilon_2 = 0$ below the bandgap, Ferlauto's E_t parameter should equal E_g and $E_1 = 0$ (accomplished with $E_u \rightarrow 0$). In (5.39), this can be accomplished by setting $E_t = 0$. In either case, the seven parameters describing ε_2 are now reduced to the common five parameters we listed in the previous paragraph. Table 5.8 provides an overview of the Cody-Lorentz equation.

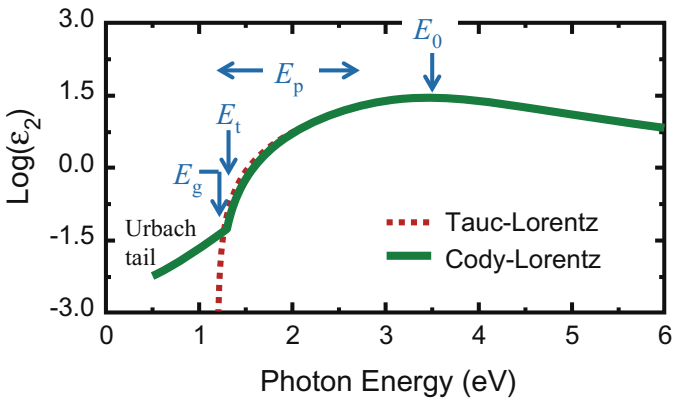

Fig. 5.16 Shape of Cody-Lorentz with parameters

jhilfiker@jawoollam.com

Table 5.8 Details of the Cody-Lorentz equation

Cody-Lorentz equation	
# of free parameters	8 or 6*
for $\varepsilon_{2:}$	7* [A, E_0, C, E_g, E_p, E_t, E_u] *most often used without Urbach tail: 5 [A, E_0, C, E_g, E_p]
for $\varepsilon_{1:}$	1 [$\varepsilon_1(\infty)$]
Primary applications:	Amorphous semiconductors and dielectrics

5.3.9 Critical Point Models

For crystalline or polycrystalline semiconductors, the dielectric function can have a very complex shape, especially in the spectral region near critical points [3, 6]. A few models have been developed to describe these specific shapes, including the critical point parabolic band (CPPB), those of Adachi, and the parametric semiconductor (PSEMI) functions.

The CPPB function [21–24] models the shape of the dielectric function near critical points using five parameters: amplitude A, phase projection factor θ, threshold energy E_g, broadening parameter Γ, and exponent n:

$$\varepsilon(E) = \varepsilon_1(E) + i\varepsilon_2(E) = C - Ae^{i\theta}(E - E_g + i\Gamma)^n \quad \text{for } n = \pm\frac{1}{2} \tag{5.40a}$$

$$\varepsilon(E) = \varepsilon_1(E) + i\varepsilon_2(E) = C - Ae^{i\theta}\ln(E - E_g + i\Gamma) \quad \text{for } n = 0 \tag{5.40b}$$

where the exponent n has three discrete values: −½, 0, or +½ for one dimensional (1-D), two dimensional (2-D) and three dimensional (3-D) critical points, respectively. Discrete excitons with a Lorentzian line-shape are represented by $n = -1$. Equation (5.40a) can be rewritten to resemble the form of a Lorentz oscillator, with $\mu = -n$, and some rescaling of Γ and A as:

$$\varepsilon(E) = \varepsilon_1(E) + i\varepsilon_2(E) = \varepsilon_1(\infty) + Ae^{i\theta}\left(\frac{\Gamma}{2E_g - 2E - i\Gamma}\right)^{\mu} \quad \text{for } \mu \neq 0 \tag{5.41a}$$

The CPPB functions are not very useful for fitting SE spectra directly, as the functions produce unphysical shapes with negative ε_2 occurring at some photon energies. They were developed to fit derivative or modulation spectra, in which case they can be successfully applied to locate the critical point features in semiconductors. Table 5.9 provides an overview of the CPPB functions.

Adachi [25, 26] developed four functions that describe the dielectric functions at semiconductor critical points, which he refers to as Model Dielectric Functions (MDFs). The different functions refer to the type of 3-D critical point based on the joint density of states near the corresponding electronic transition [3, 6]:

jhilfiker@jawoollam.com

Table 5.9 Details of the critical point parabolic band functions

CPPB equations	
# of free parameters	6
for $\varepsilon_{2:}$	5 [A, E_g, Γ, θ, n]
for $\varepsilon_{1:}$	1 [$\varepsilon_1(\infty)$]
Primary applications:	Used to fit derivative spectra of crystalline semiconductors

$$\varepsilon_{CPM0} = \varepsilon_1(E) + i\varepsilon_2(E) = \frac{A}{E_0^{1.5}\chi'^2} \cdot \left[2 - \sqrt{1+\chi'} - \sqrt{1-\chi'}\right] \tag{5.42a}$$

$$\varepsilon_{CPM1} = \varepsilon_1(E) + i\varepsilon_2(E) = \frac{-A}{\chi'^2} \cdot \ln\left[1-\chi'^2\right] \tag{5.42b}$$

$$\varepsilon_{CPM2} = \varepsilon_1(E) + i\varepsilon_2(E) = \frac{-A}{\chi''^2} \cdot \ln\left[1-\chi''^2\right] \tag{5.42c}$$

$$\varepsilon_{CPM3} = \varepsilon_1(E) + i\varepsilon_2(E) = \frac{A}{E_0^{1.5}\chi''^2} \cdot \left[2 - \sqrt{1+\chi''} - \sqrt{1-\chi''}\right] \tag{5.42d}$$

where

$$\chi' = (E + i\Gamma)/E_0 \tag{5.43a}$$

and

$$\chi'' = (E_0 - E + i\Gamma)/E_0 \tag{5.43b}$$

Again, it is possible to produce unphysical shapes with these oscillators and their primary applications are either modeling dielectric functions near the critical point energies, or fitting derivative spectra. See Schubert et al. [27] for an example of their use. Table 5.10 provides an overview of the Adachi equations.

Herzinger and Johs developed the parametric semiconductor (PSEMI) model, also referred to as the Gaussian-Broadened Polynomial Superposition (GBPS) parametric dispersion model, as a highly-flexible functional shape with KK

Table 5.10 Details of the Adachi equations

Adachi equations	
# of free parameters	4
for $\varepsilon_{2:}$	3 [A, E_0, Γ]
for $\varepsilon_{1:}$	1 [$\varepsilon_1(\infty)$]
Primary applications:	Crystalline semiconductors and fitting derivative spectra

jhilfiker@jawoollam.com

consistent properties to describe semiconductor critical points [3, 28–31]. While extremely flexible, it is also very complicated with up to 12 variable parameters to describe each critical point. The mathematical details are beyond the scope of this chapter, but can be found in the references listed. The primary advantage of this model is that it allows precise control of the ε_2 absorption shape. Figure 5.17 shows one example shape for a single PSEMI oscillator. It is based on the connection of four Gaussian broadened polynomials—two above the center energy E_c and two below—shown as F_I, F_{II}, F_{III}, and F_{IV}. There are five controllable energies; the critical point energy E_c, the minimum (left) and maximum (right) energies, E_L and E_R, and relative mid-point energies on the left and right sides, E_{ML} and E_{MR}. The E_L and E_R positions define where absorption begins and ends on the left and right sides of the oscillator, respectively. The E_{ML} and E_{MR} define the mid-points where two outer polynomials connect to the two inner polynomials. As shown in the figure, E_{ML} and E_{MR} are defined by their relative position between the min/max energies and the center energy. Thus, $E_{MR} = 0.8$ is at an energy position 80% of the distance from E_R toward E_c. The mid-point connections of polynomials is further controlled by relative amplitudes A_{ML} and A_{MR} and coefficients for the 2nd order terms in the polynomials, O_{2L} and O_{2R}. Finally, there is even the possibility of a discontinuity, *Disc*, between the left and right polynomials, positioned at the center energy. The values shown in Fig. 5.17 are for a PSEMI oscillator representing the E_1 critical point of a semiconductor.

The wide variety of PSEMI oscillator shapes is demonstrated in Fig. 5.18 where six different functions are summed to describe the ε_2 shape for CdTe. Each PSEMI oscillator maintains Kramers-Kronig consistency and ε_1 is calculated via (5.5a). The Gaussian broadened line shapes allow each oscillator to go to zero at E_L and E_R, which is a key advantage when describing materials close to their bandgap. In fact, the PSEMI is especially useful for describing the onset of absorption in direct bandgap materials, as demonstrated with "PSEMI1" in Fig. 5.18. Some of the key advantages for the PSEMI are that ε_2 remains positive and can go to zero to maintain a transparent region.

Because it is a highly flexible curve, the PSEMI is generally not a unique model. The final parameter values depend upon how the various oscillators are initially

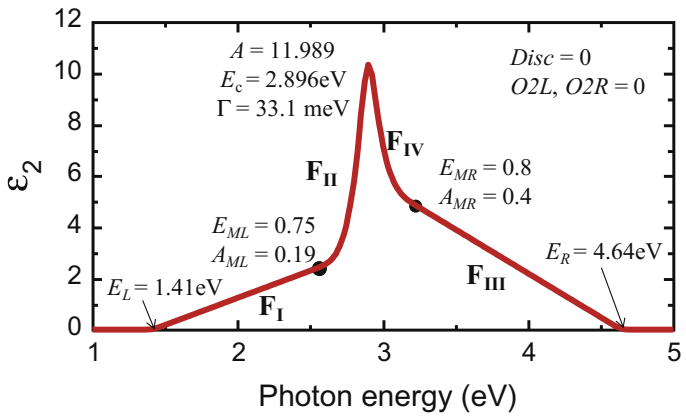

Fig. 5.17 PSEMI oscillator representing the E_1 critical point. F_I, F_{II}, F_{III}, and F_{IV} are the four polynomials connected at the two mid-point energies as well as the center energy

jhilfiker@jawoollam.com

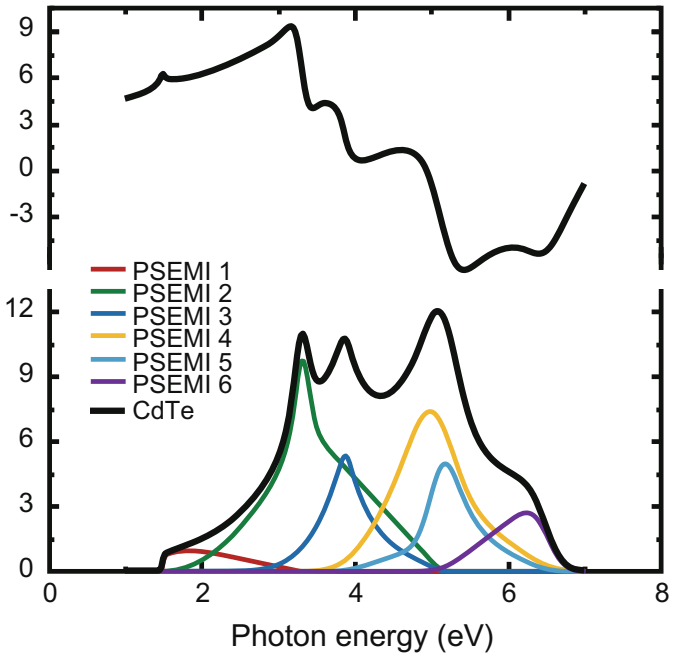

Fig. 5.18 Example Material using PSEMI for direct-bandgap material (CdTe)

configured, which means that more than one PSEMI model can produce essentially the same dielectric function and equally good fits to the data, even though they have different parameters. For this reason, one should be cautious when comparing PSEMI parameters from one model to another.

The PSEMI model's primary contribution to the understanding of the physical properties of a material is in the optical constants it generates, not the internal parameters that define the model. The PSEMI parameter values have no direct physical relationship to critical point parameters, such as energy and broadening, that one might obtain from a derivative or other type of analysis. However, the optical function generated by the PSEMI model can be subjected to a derivative analysis. Figure 5.19 shows the seven PSEMI oscillators representing the critical points of GaAs.

The primary drawback of this model is its complexity; its effective use generally requires some study and practice. Also, its parameters can be strongly correlated to other parameters within the same model. These difficulties can be overcome, and for certain situations this model is worth the time and effort. It is especially helpful for direct bandgap materials, such as CdTe, as shown in Fig. 5.18, where each individual PSEMI function is shown along with the final dielectric functions produced by the sum of six functions. Table 5.11 provides an overview of the PSEMI equations.

jhilfiker@jawoollam.com

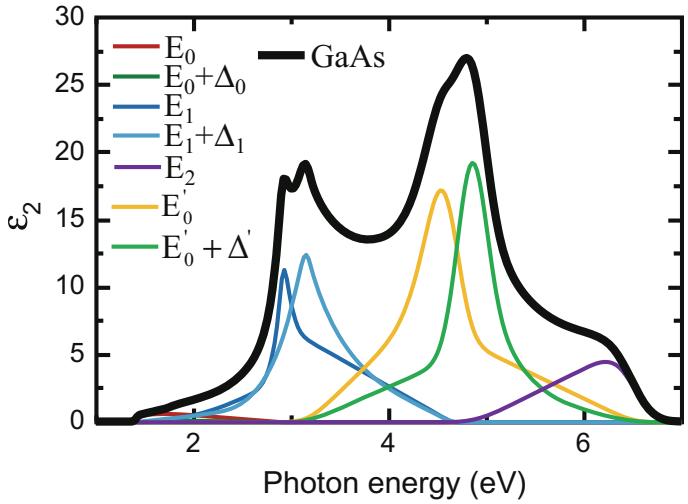

Fig. 5.19 GaAs ε_2 showing contributions of all 7 PSEMI oscillators, representing the 7 critical points

Table 5.11 Details of the parametric semiconductor equations

PSEMI equation	
# of free parameters	13
for $\varepsilon_{2:}$	12 [A, E_c, Γ, E_L, $E_{R,}$ E_{ML}, E_{MR}, A_{ML}, $A_{MR,}$ O_{2L}, O_{2R}, and Disc]
for $\varepsilon_{1:}$	1 [$\varepsilon_1(\infty)$]
Primary applications:	Crystalline semiconductors

5.3.10 Polynomials, Splines and B-Spline

Often, we wish to match our experimental SE data to accurately determine the optical functions of our material, but we are not sure which type of dispersion equation is suitable. We could adopt a direct fit, where the optical constants are independently varied at each wavelength to best match the measured SE data. However, this is highly inefficient and may produce noisy or even physically implausible results. For this reason, we prefer to choose a dispersion equation. If we are not concerned with the underlying physical phenomena that produced the optical functions, we could choose *any* equation with the ability to describe a smooth spectral curve such that a few "free" parameters adjust the shape to describe the optical functions. One such equation is a polynomial, which is shown to degree m as:

$$p_m(x) = a_m x^m + a_{m-1}x^{m-1} + \cdots + a_1 x + a_0 \tag{5.44}$$

where the a values are the real coefficients of the polynomial. The degree of the polynomial is associated with the highest power of x, with common lower degrees

jhilfiker@jawoollam.com

such as 1, 2, 3 and 4 corresponding with linear, quadratic, cubic, and quartic equations, respectively. We can rewrite (5.44) for use with spectroscopic ellipsometry versus wavelength:

$$p_m(\lambda) = a_m\lambda^m + a_{m-1}\lambda^{m-1} + \cdots + a_1\lambda + a_0 \tag{5.45}$$

or versus photon energy:

$$p_m(E) = a_m E^m + a_{m-1}E^{m-1} + \cdots + a_1 E + a_0 \tag{5.46}$$

In each of these equations, the function p could stand for any of the optical functions that we wish to describe: n, k, ε_1, or ε_2. In fact, for an absorbing material, we may need to use two separate equations, one for the real function and one for the imaginary function. As an example, the Cauchy dispersion relationship of (5.14a) can be written in terms of energy as a quartic polynomial:

$$n(E) = A + B\left(\frac{E}{1.24}\right)^2 + C\left(\frac{E}{1.24}\right)^4 \tag{5.47}$$

While polynomials work well for the transparent region which exhibits normal dispersion, it is more difficult to describe the anomalous dispersion without using polynomials of a much higher degree. A more flexible solution is the use of a spline function. The spline divides the total wavelength range into intervals with a simple function, such as a polynomial, described over each interval. With the spline, the interval size can be increased or decreased depending on the variation required over each spectral range. Splines offer the advantage of combining polynomials over regions of energy or wavelength in a piecewise continuous manner. When combining at each end-point, we wish the curves to remain continuous, which places limits on the end-points of each function. In fact, we typically desire more than just continuity from one function to the next. The type of spline is designated by the degree of the polynomials used within each function. Given a function consisting of a spline of degree k, we can enforce continuity not only on the function but also on its derivatives, up to $k - 1$. Thus, the lower order splines are not very useful for optical functions because we can't make their derivatives continuous at the joining points.

The most commonly encountered spline is cubic (polynomial degree = 3) because this allows continuity of the function, its slope (1st derivative), and its curvature (2nd derivative). The interval of each polynomial is delineated by "knots", which are the positions, t, along the wavelength or energy axis. The knot positions can be equally spaced or can have varied spacing, as shown in Fig. 5.20.

The basis-spline (b-spline) offers an interesting alternative for describing the optical functions of a material [32]. Rather than joining curves that are described for each segment, the b-spline sums individual basis functions to construct the final curve. An example basis function is shown in Fig. 5.21. Each individual basis

jhilfiker@jawoollam.com

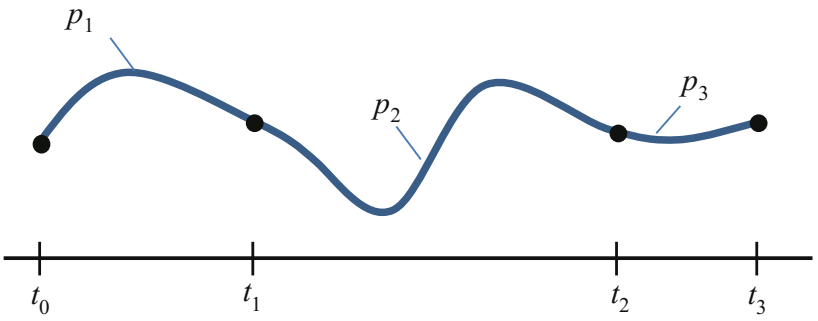

Fig. 5.20 Spline consisting of three polynomials (p) varying between knot positions (t) connected to maintain a smooth, continuous curve

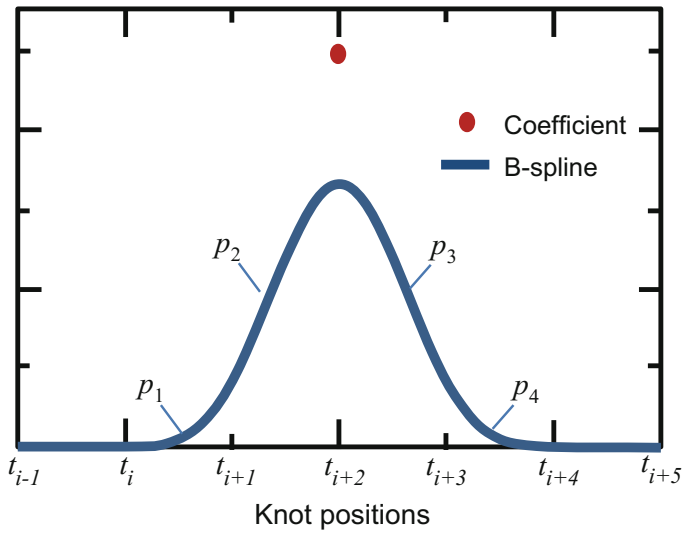

Fig. 5.21 A single 3rd degree basis function shows the four polynomial sections used to create a single shape, with the overall amplitude controlled by the coefficient of the basis function

function is constructed from multiple polynomials; in this case four polynomials are required to describe the 3rd degree basis function.

The basis function can be written in recursive form as:

$$B_i^0(x) = \begin{cases} 1 & t_i \le x < t_{i+1} \\ 0 & \text{otherwise} \end{cases} \tag{5.48a}$$

$$B_i^k(x) = \left(\frac{x - t_i}{t_{i+k} - t_i}\right) B_i^{k-1}(x) + \left(\frac{t_{i+k+1} - x}{t_{i+k+1} - t_{i+1}}\right) B_{i+1}^{k-1}(x) \tag{5.48b}$$

where "k" is the degree of the b-spline. These equations describe a single basis function. However, multiple basis functions, or "spline components" are summed to describe the overall shape of our basis-spline function, with coefficients, c, to adjust each spline components amplitude:

jhilfiker@jawoollam.com

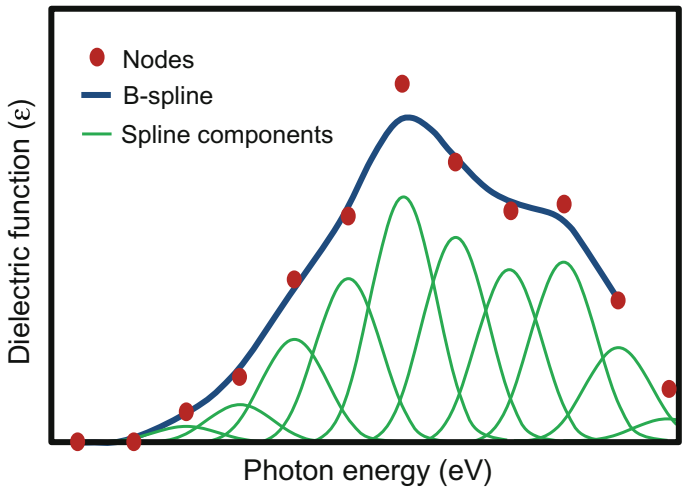

Fig. 5.22 Example of a b-spline curve to describe the dielectric function of a material with a summation of basis functions, each controlled by their node amplitude

$$S(x) = \sum_{i=1}^{n} c_i B_i^k(x) \tag{5.49}$$

Figure 5.22 shows the individual spline components summed together to form the basis-spline curve describing ε_2 of a material. Each basis function maintains its specific shape and is controlled by an associated coefficient, shown here as the nodes. The final function does not have to go through each node, but the node amplitude (amplitude of the spline coefficient) adjusts the general shape of the curve in a local region. The spacing between nodes (which also adjusts the corresponding "knot" spacing) can be reduced to increase control over the shape of the final b-spline curve. This introduces more "free" parameters, which are the individual coefficients or node values for each basis function. In this manner, the b-spline can be optimized by increasing or decreasing the node spacing based on the variability of the optical function it is being used to describe.

Dielectric functions are usually represented by a 3rd order recursive basis polynomial function [32]. The 3rd order b-spline curves have many desirable properties [33] for modeling dielectric functions:

- The function and its 1st and 2nd order derivatives are smooth and continuous.
- Each basis function affects only the "local" shape of the curve. For example, changing a node amplitude in the UV does not affect the curve in the NIR.
- B-spline curves exhibit a "convex hull" property, where the summed function can't exceed the highest or lowest node amplitude. This allows the b-spline to remain non-negative as long as all spline coefficients (nodes) are ≥ 0, thus avoiding non-physical negative ε_2 values. This is demonstrated in Fig. 5.23.
- Since the basis functions depend only on the node positions, the node amplitudes which define the resulting curve are linearly independent, which greatly increases computation efficiency.

jhilfiker@jawoollam.com

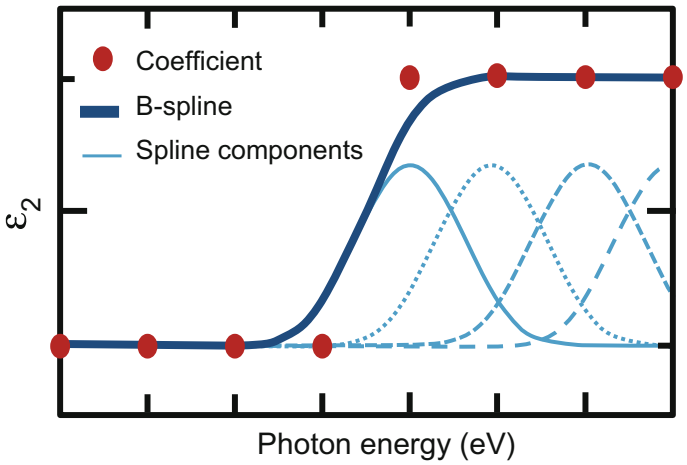

Fig. 5.23 Example b-spline showing the convex hull property where the final b-spline summation does not exceed the lower or upper node coefficient values. This is especially useful when describing the ε_2 curve such that it will not go to negative values

- The KK integral can be applied to the b-spline recursion formula to generate KK consistent basis functions. In other words, the ε_1 curve can be defined by the KK transform of ε_2.

When applying b-splines to the optical functions of materials, there are generally two options:

- The first option is to generate separate b-spline curves for the real and imaginary components, as shown in Fig. 5.24 for an organic material. The total number of free parameters is slightly more than twice the number of node positions. Here, the number of free parameters is tied to the total number of nodes and efficient minimization of "free" parameters is achieved by optimizing the node spacing—even allowing different spacing for different spectral regions.
- The second option is to use a single b-spline to describe the imaginary function, and then calculate the real function using the KK integral. This significantly reduces the number of free parameters, as only one of the curves has free parameters at every node. In this latter case, care must be taken with any b-spline nodes that are located outside the investigated spectral range, as these

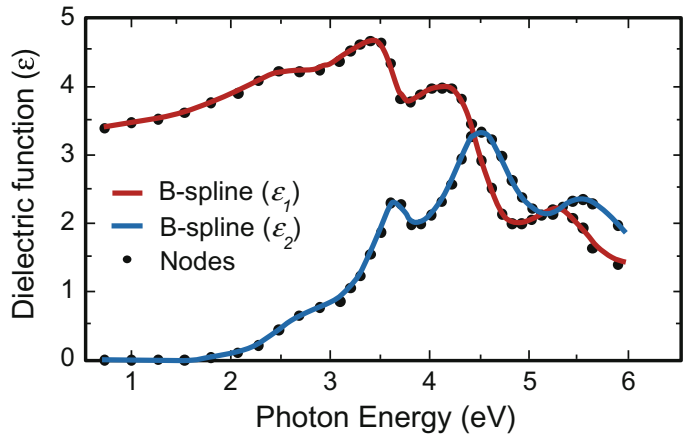

Fig. 5.24 Example of b-spline for organic material, where separate b-spline curves are used to describe ε_1 and ε_2

jhilfiker@jawoollam.com

Table 5.12 Details of the basis-spline functions

B-spline	
# of free parameters	~2 × number of nodes (non KK) ~1 × number of nodes (KK)
for $\varepsilon_{2:}$	~1 × number of nodes
for $\varepsilon_{1:}$	~1 × number of nodes (non KK) 1–3 (KK)
Primary applications:	Organics, dielectrics, semiconductors, and metals

will also affect the KK integration. An offset and "poles" may be added to correct for absorption features outside the investigated spectral range. For materials with a transparent region, it is also very efficient to enforce this transparency by setting the nodes for ε_2 equal to zero over transparent spectral region. Table 5.12 provides an overview of the b-spline functions.

References

1. H. Fujiwara, *Spectroscopic Ellipsometry: Principles and Applications* (Wiley, West Sussex, UK, 2007), pp. 347–348
2. J.D. Jackson, *Classical Electrodynamics*, 3rd edn. (Wiley, New York, 1999)
3. R.W. Collins, A.S. Ferlauto, in *Handbook of Ellipsometry*, ed. by H.G. Tompkins, E.A. Irene (William Andrew, New York, 2005). pp. 93–235, Chap. "Optical Physics of Materials"
4. H. Fujiwara, *Spectroscopic Ellipsometry: Principles and Applications* (Wiley, West Sussex, UK, 2007), pp. 357–360
5. S. Logothetidis, *Ellipsometry of Functional Organic Surfaces and Films,* ed. by K. Hinrichs, K.-J. Eichorn, (Springer, Berlin, 2014). pp. 173–195, Chap. "Polymer Blends and Composites"
6. P.Y. Yu, M. Cardona, *Fundamentals of Semiconductors: Physics and Materials Properties* (Springer, Berlin, 2001)
7. A. Röseler, *Infrared Spectroscopic Ellipsometry* (Akademie-Verlag, Berlin, 1990)
8. M. Schubert, *Infrared Ellipsometry on Semiconductor Layer Structures: Phonons, Plasmons, and Polaritons* (Springer, Berlin, 2004)
9. W. Sellmeier, Annalen der Physik und Chemie **143**, 271 (1871)
10. Schott Glass Catalog, p. 69 (2014)
11. C.M. Herzinger, B. Johs, W.A. McGahan, J.A. Woollam, W. Paulson, J. Appl. Phys. **83**, 3323 (1998)
12. L. Cauchy, Bull. Des. Sc. Math. **14**, 9 (1830)
13. F. Urbach, Phys. Rev. **92**, 1324 (1953)
14. F. Wooten, *Optical Properties of Solids* (Academic Press, New York, 1972)
15. C. Kittel, *Introduction to Solid State Physics*, 5th edn. (Wiley, New York, 1976)
16. T.E. Tiwald, D.W. Thompson, J.A. Woollam, W. Paulson, R. Hance, Thin Solid Films **313–314**, 661 (1998)
17. D. De Sousa Meneses, M. Malki, P. Echegut, J. Non-Cryst. Solids **351**, 769–776 (2006)
18. K.-E. Peiponen, E.M. Vartiainen, Phys. Rev. B **44**, 8301 (1991)
19. G.E. Jellison, Jr., F.A. Modine, Appl. Phys. Lett. **69**, 371 (1996); Erratum, Appl. Phys. Lett. **69**, 2137 (1996)

jhilfiker@jawoollam.com

20. A.S. Ferlauto, G.M. Ferreira, J.M. Pearce, C.R. Wronski, R.W. Collins, Xunming Deng, Gautam Ganguly, J. Appl. Phys. **92**, 2424 (2002)
21. M. Cardona, *Solid State Physics*, ed. by F. Seitz, D. Turnbull, H. Ehrenreich (Academic, New York, 1969). Suppl. 11 "Modulation Spectroscopy"
22. D.E. Aspnes, *Handbook on Semiconductors*, vol. 2, ed. by M. Balkanski (North Holland, 1980), pp. 125–127, Chap. "Modulation Spectroscopy/Electric Field Effects on the Dielectric Function of Semiconductors"
23. P. Lautenschlager, M. Garriga, L. Vina, M. Cardona, Phys. Rev. B **36**, 4821 (1987)
24. P. Lautenschlager, M. Garriga, S. Logothetidis, M. Cardona, Phys. Rev. B **35**, 9174 (1987)
25. S. Adachi, Phys. Rev. B **35**, 7454 (1987)
26. S. Adachi, J. Appl. Phys. **66**, 6030 (1989)
27. Mathias Schubert, Tino Hofmann, Bernd Rheinländer, Ines Pietzonka, Torsten Sass, Volker Gottschalch, John A. Woollam, Phys. Rev. B **60**, 16618 (1999)
28. B. Johs, C.M. Herzinger, J.H. Dinan, A. Cornfeld, J.D. Benson, Thin Solid Films **313–314**, 137 (1998)
29. US Patent #5,796,983, Dielectric function parametric model, and method of use
30. B. Johs, J.A. Woollam, C.M. Herzinger, J. Hilfiker, R. Synowicki, C.L. Bungay, SPIE Proc. **CR72**, 29 (1999)
31. Y.S. Ihn, T.J. Kim, T.H. Ghong, Y.D. Kim, D.E. Aspnes, J. Kossut, Thin Solid Films **455–456**, 222 (2004)
32. B. Johs, J.S. Hale, Phys. Stat. Sol. A **205**, 715 (2008)
33. E. Cheney, D. Kincaid, *Numerical Mathematics and Computing*, 3rd edn. (Brooks/Cole Publishing, 1994)

jhilfiker@jawoollam.com